Recognition Sequence Design for Peptidyl Modulators of β-Amyloid Aggregation and Toxicity†

Monica M. Pallitto,‡ Jyothi Ghanta,§ Peter Heinzelman,‡ Laura L. Kiessling,§ and Regina M. Murphy*,‡

Departments of Chemical Engineering and Chemistry, University of Wisconsin, Madison, Wisconsin 53706

Received September 1, 1998; Revised Manuscript Received January 5, 1999

ABSTRACT: β-Amyloid (Aβ), the primary protein component of Alzheimer's plaques, is neurotoxic when aggregated into fibrils. We have devised a modular strategy for generating compounds that inhibit Aβ toxicity, based on linking a recognition element for Aβ to a disrupting element designed to interfere with Aβ aggregation. One such compound, with the 15−25 sequence of Aβ as the recognition element and a lysine hexamer as the disrupting element, altered Aβ aggregation kinetics and protected cells from Aβ toxicity [Ghanta et al. (1996) *J. Biol. Chem. 271*, 29525]. To optimize the recognition element, peptides of 4−8 residues composed of overlapping sequences within the 15−25 domain were synthesized, along with hybrid compounds containing those recognition sequences coupled to a lysine hexamer. None of the recognition peptides altered Aβ aggregation kinetics and only two, KLVFF and KLVF, had any protective effect against Aβ toxicity. The hybrid peptide KLVFF-KKKKKK dramatically altered Aβ aggregation kinetics and aggregate morphology and provided significantly improved protection against Aβ toxicity compared to the recognition peptide alone. In contrast, FAEDVG-KKKKKK possessed only modest inhibitory activity and had no marked effect on Aβ aggregation. The scrambled sequence VLFKF was nearly as effective a recognition domain as KLVFF, suggesting the hydrophobic characteristics of the recognition sequence are critical. None of the cytoprotective peptides prevented Aβ aggregation; rather, they increased aggregate size and altered aggregate morphology. These results suggest that coupling recognition with disrupting elements is an effective generalizable strategy for the creation of Aβ inhibitors. Significantly, prevention of Aβ aggregation may not be required for prevention of toxicity.

The progressive, degenerative disease of the brain known as Alzheimer's disease (AD[1] affects approximately 4 million Americans. The presence of amyloid plaques is considered one of the defining pathological feature of Alzheimer's disease. The primary protein component of these plaques is β-amyloid (Aβ) peptide, deposited as amyloid fibrils. Aβ is a 39−43 amino acid fragment from the membrane amyloid precursor protein (APP). The Aβ region of APP includes 28 residues that reside outside the membrane and 11−15 residues in the transmembrane domain (*1*); therefore Aβ is amphiphilic. It is widely hypothesized, but not universally accepted, that the conversion of Aβ to fibrils is a causative event in the onset of AD (*2*, *3*). This hypothesis is supported in part by transgenic animal studies (*4*−*7*) and by numerous in vitro studies showing that Aβ is toxic to cells in culture (*8*−*10*). AD has been linked to either increased production or increased deposition of Aβ, and there is evidence that the deposition of Aβ predates other AD pathological events (*11*, *12*).

The origin of the cellular toxicity of Aβ is an active area of research. A number of studies indicate that toxicity is associated with the aggregation process that converts monomeric, soluble Aβ to insoluble fibrils (*8*, *13*−*15*). If the process of aggregation confers toxicity, then appropriate therapeutic strategies include interruption of aggregation (*16*, *17*). Several small molecules, including sulfonated compounds such as Congo red or related molecules (*18*−*20*), surfactants (*21*, *22*), rifampicin and related naphthohydroquinones (*23*), the cationic aromatic compound pyronine Y (*24*), and cyclodextrin (*25*, *26*), have demonstrated in vitro activity in Aβ aggregation or Aβ toxicity assays. These compounds are unlikely to specifically target Aβ, however.

An alternative approach is to exploit the self-recognizing features of Aβ to generate molecules that can serve as aggregation inhibitors. This strategy rests on the hypothesis that a fragment of Aβ should selectively bind Aβ, thereby occupying a target site for aggregation and directly interfering with fibril formation and growth. Experimental support for this idea has recently appeared. Tjernberg et al. (*27*) screened several short peptide segments for binding to Aβ, and observed strongest interactions with KLVFF, residues 16−20 of Aβ, or slightly longer peptides containing this sequence. KLVFF, along with D-amino acid analogues lflrr

† Financial support was provided by an Alzheimer Disease Research grant from the American Health Assistance Foundation, the Alzheimer's Association, and an NIH Molecular Biophysics Training Grant 5T32 GM08293-09 (M.M.P.).

* To whom correspondence should be addressed at 1415 Engineering Dr., Madison, WI 53706. Tel (608) 262-1587; e-mail murphy@che.wisc.edu.

‡ Department of Chemical Engineering.

§ Department of Chemistry.

[1] Abbreviations: Aβ, β-amyloid; AD, Alzheimer's disease; APP, amyloid precursor protein; EDTA, ethylenediaminetetraacetic acid; HPLC, high-pressure liquid chromatography; MTT, 3-(4,5-dimethylthiazol-2-yl)-2,5-diphenyltetrazolium bromide; PBS, phosphate-buffered saline; PBSA, phosphate-buffered saline with azide; TFA, trifluoroacetic acid; ThT, thioflavin T.

10.1021/bi982119e CCC: $18.00
Published on Web 03/08/1999

and yflrr, inhibited fibril formation, as assessed by electron microscopy (*27*, *28*). The octapeptide QKLVTTAE, with substitutions for the two Phe residues at positions 19 and 20, inhibited fibril formation at a 10-fold molar excess, a result attributed to weak interactions between the octapeptide and monomeric Aβ (*29*). Peptides with partial homology to the central 17−21 region of Aβ but with proline substituents at key positions were designed as β-sheet breakers and were observed to convert Aβ fibrils to amorphous aggregates and inhibit Aβ toxicity in vitro and in a rat brain model (*30*, *31*). Together, these studies provide evidence that molecules that can bind to Aβ may interfere with its aggregation.

We have pursued a related but distinct strategy. In this design, partial homologues of Aβ are used as a means to introduce a specific binding domain ("recognition element") into an inhibitory compound, but fibril disruption is augmented through addition of a separate domain, the "disrupting element". This modular design allows greater flexibility, since the domains of the compound can be optimized independently for their binding and disrupting functionality. The successful implementation of this strategy has been described (*32*). In that example, the recognition element corresponded to the 15−25 sequence of Aβ, and the disrupting element was chosen to be a polar, charged sequence of lysines, appended to the C-terminus of the recognition sequence. This hybrid compound protected PC-12 cells from Aβ toxicity and engendered striking changes in the aggregation kinetics of Aβ solutions.

The goals of the work reported here were to (1) further explore the design requirements for Aβ recognition, (2) determine the necessity and function of the lysine hexamer disrupting element, and (3) define the relationship between the influence of inhibitors on aggregation and on toxicity.

MATERIALS AND METHODS

Peptide Synthesis. Aβ(1−39) was purchased from AnaSpec, Inc. (San Jose, CA). The peptide sequence, DAEFRHDSGYEVHHQKLVFFAEDVGSNKGAIIGLMVGGV, is homologous to the first 39 residues of native Aβ. Purity and identity were assessed by amino acid analysis, mass spectrometry, and reverse-phase HPLC; the reported purity was >95% and the reported molecular weight was 4231 (theoretical molecular weight of 4232). All other peptides were synthesized by solid-phase peptide synthesis using Fmoc-protected amino acids. The crude peptides were purified by reverse-phase HPLC on a C18 Vydac column with linear gradients of acetonitrile/water with 0.1% TFA. The mass of the purified peptides was analyzed by mass spectrometry. Peptides were stored as lyophilized powders at −70 °C. All other chemicals, unless otherwise noted, were purchased from Sigma (St. Louis, MO).

Analytical Ultracentrifugation. Peptide solutions at ∼0.5 mg/mL in phosphate-buffered saline (PBS; 0.01 M K_2HPO_4/KH_2PO_4 and 0.14 M NaCl, pH 7.4) were injected into 1.2 cm path length cells and then centrifuged at 50 000−60 000 rpm in a Beckman Optima XL-A ultracentrifuge for 20−24 h. Absorbance A at 230 or 257 nm was measured as a function of radial position r and the data were fitted to

$$\frac{\mathrm{d} \ln A}{\mathrm{d}r^2} = \frac{M(1 - \upsilon\rho)\omega^2}{2RT} \qquad (1)$$

to obtain the molecular weight M. The specific volume υ of the peptides was calculated from the amino acid sequence.

Cellular Toxicity. Lyophilized Aβ was dissolved in 0.1% TFA at 10 mg/mL. All other peptides were dissolved directly into sterile-filtered PBS that contained streptomycin and penicillin to prevent microbial growth. Peptide concentration in stock solutions was typically 2.5 mg/mL. Aβ was diluted 20-fold into sterile-filtered PBS to 0.5 mg/mL or mixed with the peptide solutions to a final Aβ concentration of 0.5 mg/mL and a peptide:Aβ molar ratio of 2:1 or 1:1 unless otherwise indicated. Solutions were incubated quiescently for 1 week at room temperature. PC-12 cells (ATCC) were grown in medium containing 85% RPMI 1640, 5% fetal bovine serum, 10% heat-inactivated horse serum, 3.6 mM L-glutamine, and antibiotics, in a humidified incubator at 37 °C and 5% CO_2. Cells were harvested from T-flasks with trypsinization (0.05% trypsin and 0.4 mM EDTA), resuspended in medium, and plated into 96-well plates at 10 000−15 000 cells/well. Plates were incubated for 24 h to allow cells to attach. Aβ or peptide−Aβ solutions were diluted 5-fold into medium and incubated at room temperature for 1 day, then medium from attached cells was removed and replaced with medium containing Aβ or peptide−Aβ mixtures. After 24 h of incubation at 37 °C, 10 μL of MTT (5 mg/mL in RPMI medium without phenol red) was added to each well. After 4 h, 100 μL of 50% dimethyl formamide/20% sodium dodecyl sulfate, pH 4.7, was added and the plates were incubated overnight, and absorbance at 580 nm was read the next day on a Labsystems Uniskan II microplate reader. Percent cell viability was determine by dividing absorbance of the sample by the absorbance of a control (cells treated in an identical manner but without Aβ). Averages from 6 replicate wells were used for each sample and control.

Laser Light Scattering. PBSA [PBS with 0.02% (w/v) NaN_3, pH 7.4] was double-filtered through 0.22 μm filters. Aβ was dissolved in 0.1% TFA to a concentration of 10 mg/mL and then diluted 20-fold into filtered PBSA or PBSA containing synthesized peptides. The molar ratio of peptide:Aβ was 2:1 unless otherwise indicated. The pH was adjusted to 7.4 with 0.5 M NaOH and then the solution was filtered through 0.45 μm filters directly into a cleaned light-scattering cuvette placed in a bath of the index-matching solvent decahydronaphthalene, which was temperature-controlled to 25 °C. Dynamic light scattering data were taken with a Lexel argon ion laser for illumination and a Malvern 4700 system, as described in more detail elsewhere (*33*). Autocorrelation data at 90° scattering angle were collected several times over the course of ∼6 h, as described in more detail elsewhere (*33*). Data were fit to a third-order cumulants expression (*34*) to derive an average apparent hydrodynamic diameter.

After 24 h, static light scattering measurements were taken with the same samples and apparatus: briefly, the scattered light intensity at 22 angles from 20° to 140° was collected for 10 s; each measurement was repeated 10 times and averaged. Average scattered intensity of the buffer was measured in the same manner and subtracted from the sample scattering intensity; the result was then normalized by using the scattering intensity of the reference solvent toluene to obtain the Rayleigh ratio $R_s(q)$ as a function of scattering vector q, where $q = 4\pi n/\lambda_0 \sin(\theta/2)$, n is the refractive index of the solvent, λ_0 is the wavelength of the incident beam in

vacuo, and θ is the scattering angle. Data were analyzed as described in greater detail elsewhere (*35*). Briefly, the data were plotted in the Kratky format, $q^2R_s(q)/Kc$ [$= q^2M_wP(q)$] versus q, where c is the peptide concentration, $K = 4\pi^2n^2(dn/dc)^2/N_A\lambda_0^4$, dn/dc is the refractive index increment, N_A is Avogadro's number, M_w is the weight-average molecular weight, and $P(q)$ is the particle scattering factor, which is a function of particle shape. Second virial coefficient correction terms were ignored. The Kratky plot is a convenient means for observing linear vs branched structures for particles with characteristic dimensions on the order of the wavelength of the incident beam (*36*). A smoothly rising plot with a plateau at intermediate q is typical of semiflexible linear chains, whereas a "bump" in the graph at intermediate q is characteristic of a branching structure. Two alternative models of particle shape, semiflexible (wormlike) chain and semiflexible (wormlike) star, were used to fit the data. The semiflexible chain model describes a linear chain with total contour length L_c and Kuhn statistical segment length l_k (a measure of the stiffness of the chain, equal to two times the persistence length). $P(q)$ for semiflexible wormlike chains is

$$P(q) = \frac{2}{L_c^2}\int_0^{L_c}(L_c - t)\phi(t,l_k,q)\,dt \qquad (2)$$

where the function $\phi(t,l_k,q)$ has been described elsewhere (*34*, *37*). We have shown previously that this model is a good description of Aβ fibrils (*34*, *35*). The continuous wormlike star model describes a branched particle with a center from which emanate f semiflexible chains of equal length. $P(q)$ for the continuous wormlike star model is a function of l_k, the contour length of one arm $L_{c,a}$, and the number of branches f (*38*):

$$P(q) = \frac{1}{fL_{c,a}^2}\{2(2-f)\int_0^{L_{c,a}}(L_{c,a} - x)\phi\,dx + (f-1)\int_0^{2L_{c,a}}(2L_{c,a} - x)\phi\,dx\} \qquad (3)$$

M_w, l_k, L_c (or $L_{c,a}$), and, where appropriate, f were determined by nonlinear regression of the data using the parameter estimation software program GREG (39), with numerical integration to evaluate eq 2 or 3. To reduce covariances to acceptable levels, fitting was done by reparametrization to the parameter set (M_w/L_c, L_c, L_cl_k) for eq 2 or (M_w, $L_{c,a}$, $L_{c,a}l_k$, and $fL_{c,a}^{0.4}$) for eq 3. M_w was independently determined by extrapolation of Kc/R_s vs q^2 to $q^2 = 0$ (Zimm plot) and in all cases agreed to that determined by regression to the multiple parameter set within experimental error.

RESULTS

Previously we found that a hybrid compound, comprising the 15−25 sequence of Aβ as a recognition sequence with a hexameric lysine at the C-terminus as a disrupting element, was capable of protecting PC-12 cells from toxicity and of altering the aggregation kinetics of Aβ (*32*). Therefore, we examined the ability of shorter peptide segments within the 15−25 sequence of Aβ to serve as recognition elements. Several recognition peptides of 4−8 residues with overlapping sequences were synthesized and purified (Table 1). In addition, two control peptides (a scrambled sequence peptide and an *N*-acetyl-capped recognition peptide) and three additional hybrid peptides (the recognition elements 16−20 or 20−25, or the scrambled sequence 16−20S, coupled to a hexameric lysine disrupting element) were synthesized (Table 1). C-Terminal placement of the disrupting element was chosen on the basis of previous results (*32*). Analytical ultracentrifugation experiments revealed that 16−20, 18−25, and 20−25 were monomeric in PBS (molecular weights of 680 ± 10, 870 ± 30, and 720 ± 10, respectively), but 16−25 was highly aggregated. The hybrid peptide 15−25-K_6 was monomeric by analytical ultracentrifugation (molecular weight 2030 ± 20), indicating that C-terminal attachment of the lysine hexamer completely solubilized the otherwise highly aggregated Aβ fragment. Other peptides were not tested by ultracentrifugation.

Table 1: Synthesized Peptides

Name	Sequence	Theoretical Mol. Wt.	Mol. Wt. Mass Spec.	Water-soluble?
Recognition peptides				
16-19	KLVF	505.7	506.3	yes
16-20	KLVFF	652.8	653.4	yes
16-25	KLVFFAEDVG	1124.4	1125.3	no
17-20	LVFF			no
18-25	VFFAEDVG	883.0	883.5	yes
19-25	FFAEDVG	783.8	784.4	yes
20-25	FAEDVG	636.7	637.4	yes
16-20S	VLFKF	652.8	653.4	yes
cap16-20	CH_3CO-KLVFF	698.9	698.4	partially
Hybrid peptides				
16-20-K_6	KLVFFKKKKKK	1421.9	1422.0	yes
16-20S-K_6	VLFKFKKKKKK	1421.9	1421.8	yes
20-25-K_6	FAEDVGKKKKKK	1406	1405.4	yes
15-25-K_6	GQKLVFFAEDVGGaKKKKKK	2192.7	2190.3	yes

Peptide sequences within the 15−25 domain of Aβ were examined for their ability to inhibit the toxicity of Aβ(1−39) toward PC-12 cells, using the MTT reduction assay. A decrease in ability to reduce MTT is reportedly an early indicator of Aβ toxicity (*40*). None of the peptides listed in Table 1 were toxic by themselves (data not shown). Treatment of cells with aggregated Aβ at 25 μM caused a decrease in MTT reduction to about 55% of control, consistent with previously reported data (*32*). Recognition peptides from Table 1 were added at a 1:1 or 2:1 peptide:Aβ molar ratio. The resulting solution was incubated at room temperature for 1 week and then added to plated PC-12 cells. Two recognition peptides, 16−20 ($p < 0.0005$) and, to some extent, 16−19 ($p < 0.01$), prevented the decrease in MTT reduction at a 2:1 peptide:Aβ ratio (Figure 1). Recognition peptides derived from the C-terminal end of the 15−25 sequence (18−25, 19−25, and 20−25) were not protective at a statistically significant level, nor was a scrambled sequence 16−20S or the *N*-acetylated peptide cap16−20 (Figure 1). The insolubility of 16−25 in PBS precluded analysis of its effect on Aβ toxicity. When the peptide concentration was decreased to 25 μM (1:1 molar ratio), only 16−19 showed a modest protective effect at a statistically significant level ($p < 0.01$).

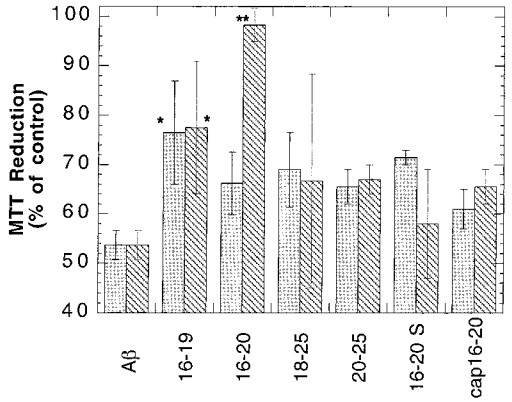

FIGURE 1: Effect of recognition peptides or 16−20 variants on cellular toxicity of Aβ solutions. Aβ at 120 μM alone or with the designated peptide was incubated for 1 week at room temperature, then diluted 5-fold, and added to plated PC-12 cells for 1 day. Cellular toxicity was assessed by the MTT assay. Each bar represents the mean ± SEM of 2−9 separate runs, with 4−6 replicates per run. Gray bars, 1:1 peptide:Aβ molar ratio; hatched bars; 2:1 peptide:Aβ molar ratio. Comparison of toxicity of Aβ + peptide to toxicity of Aβ alone: *, $p < 0.01$; **, $p < 0.0005$.

Next, the effect of hybrid peptides on Aβ toxicity was measured, to determine if attachment of the disrupting element, a lysine hexamer, to the C-terminus of the recognition elements generated compounds with increased inhibitory activities. At a 2:1 peptide:Aβ molar ratio, all four hybrid compounds provided at least partial protection against Aβ toxicity, in contrast to what was observed with the recognition peptides. At a 1:1 ratio, 20−25-K_6 was no longer protective, while the other three hybrids provided partial (15−25-K_6) or complete (16−20-K_6 and 16−20S-K_6) protection (Figure 2A). The activity of the hybrid compounds is compared to their corresponding recognition peptides in Figure 2B. At a 1:1 ratio, hybrid peptides 16−20-K_6 and 16−20S-K_6 were superior protective agents compared to the corresponding recognition peptides 16−20 or 16−20S. Although 15−25-K_6 and 20−25-K_6 were slightly more protective than their corresponding recognition peptides, the differences were not statistically significant.

We hypothesized that the differences in inhibitory activity in the biological assay would be reflected in differences in aggregation behavior. To elucidate the effect of these compounds on Aβ aggregation, mixtures of peptide and Aβ were prepared under conditions that resulted in Aβ aggregation into fibrils (*35*). The kinetics of aggregate growth were measured by dynamic light scattering. The apparent hydrodynamic diameter of Aβ aggregates in solution increased slowly with time. Mixing any of the recognition peptides with Aβ at a 2:1 peptide:Aβ molar ratio had no substantial impact on the rate of growth (Figure 3). The hybrid peptide 20−25-K_6 also did not alter Aβ aggregation kinetics. In sharp contrast, peptides 16−20-K_6, 16−20S-K_6, and 15−25-K_6 all caused marked increases in the growth kinetics. At a 2:1 peptide:Aβ molar ratio the growth rate of Aβ in the presence of 16−20-K_6 or 16−20S-K_6 was markedly greater than that of Aβ + 15−25-K_6 and was too fast to collect reliable data. Therefore, the experiment was repeated with those two hybrids at a 0.5:1 peptide:Aβ molar ratio. The growth rate for 16−20-K_6 + Aβ at the lower molar ratio was similar to that for 15−25-K_6 + Aβ at the higher molar ratio (Figure 3). For 16−20S-K_6 + Aβ, the growth rate was lower than

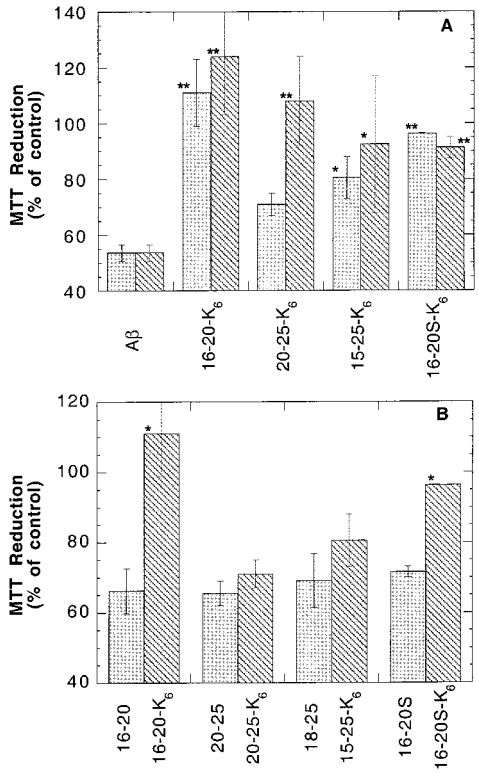

FIGURE 2: Effect of hybrid peptides on cellular toxicity of Aβ solutions. Experiments were carried out as described in the legend to Figure 1. (A) Comparison of toxicity of Aβ + hybrid peptides to toxicity of Aβ alone at a 1:1 (gray bars) and a 2:1 (hatched bars) peptide:Aβ molar ratio. *, $p < 0.005$; **, $p < 0.0005$. (B) Comparison of toxicity of Aβ + recognition peptides (gray bars) to toxicity of Aβ + hybrid peptides (hatched bars) peptides at a 1:1 molar ratio. *, $p < 0.005$.

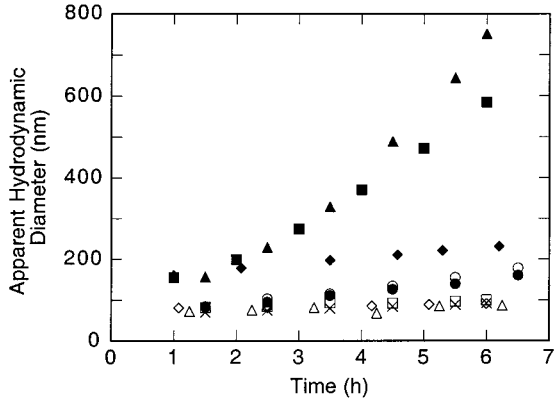

FIGURE 3: Growth kinetics of Aβ aggregates. Apparent hydrodynamic diameter of Aβ (×); Aβ with the recognition peptides 16−20 (□), 18−25 (△), 20−25 (○), or 16−20S (◇); and Aβ with the hybrid compounds 16−20-K_6 (■), 15−25-K_6 (▲), 20−25-K_6 (●), or 16−20S-K_6 (◆) was measured by dynamic light scattering at an Aβ concentration of 0.5 mg/mL (120 μM) and a 2:1 peptide:Aβ molar ratio, except for 16−20-K_6 and 16−20S-K_6, which were taken at a 0.5:1 peptide:Aβ molar ratio.

for 16−20-K_6 + Aβ but still greater than for Aβ alone (Figure 3). From these data, we conclude that the hybrid peptide 16−20-K_6 has the greatest effect on Aβ aggregation kinetics, followed by 16−20S-K_6 and then 15−25-K_6. In contrast, 20−25-K_6 does not measurably affect aggregation kinetics.

Static light scattering data were collected for the peptides alone or Aβ alone. Scattering from the peptides at ∼240 μM

Table 2: Effect of Aβ Fragments on the Size of Aβ Aggregates

sample	M_w[a] ($\times 10^6$ Da)	L_c (nm)	l_k (nm)
Aβ	8 ± 2	1300 ± 300	150 ± 50
Aβ + 20−25	11 ± 4	2400 ± 700	110 ± 40
Aβ	8 ± 1	780 ± 60	190 ± 30
Aβ + 18−25	11 ± 1	1100 ± 100	170 ± 30
Aβ + 16−20	18 ± 1	1500 ± 100	170 ± 20
Aβ	1.9 ± 0.1	230 ± 10	ND[b]
Aβ + 16−20S	3.8 ± 0.3	510 ± 30	190 ± 30

[a] Values for average molecular weight M_w, fibril length L_c, and stiffness l_k were obtained by fitting eq 2 to data in Figure 4. Each Aβ + fragment mixture should be compared with Aβ in its grouping. [b] ND = not determined. An estimate of l_k could not be extracted from the data, indicating that the fibril is sufficiently short, relative to its characteristic stiffness, to behave as a rod.

in the absence of Aβ was indistinguishable from scattering from buffer alone, indicating that these peptides do not by themselves form large aggregates (data not shown). Aβ solutions strongly scattered light, indicating the presence of large aggregates. Further analysis of the data indicated that the angular dependence of the scattering was indicative of linear semiflexible fibrils. Fitted values of the average molecular weight M_w, length L_c, and stiffness l_k of the Aβ aggregates were determined from the data and are given in Table 2. The variability in the individual data sets observed is likely due to inaccuracies in the measurement of Aβ concentration, as this variable would strongly impact the rate of aggregation as well as the analysis of the scattering data. To minimize the effects of variability and to allow for clearer assessment of any changes in aggregate size or morphology caused by the recognition or hybrid peptides, we typically compared data for peptide−Aβ mixtures with data for Aβ alone prepared from the same batch of Aβ and on the same day.

Next, the effect of recognition peptides on Aβ aggregate size was explored. Representative scattering data are presented as Kratky plots for Aβ alone or with the recognition peptides 20−25, 18−25, 16−20, and 16−20S in Figure 4. The scattering curves for Aβ + 20−25 (Figure 4A) and for Aβ + 18−25 (Figure 4B) correspond almost exactly to the curves for Aβ alone. This indicates that the peptides 20−25 and 18−25 do not affect the molecular weight, length, or shape of Aβ aggregates. Scattering curves for Aβ + 16−20 (Figure 4C) and Aβ + 16−20S (Figure 4D) retain shapes similar to that for Aβ alone but the entire curve is shifted upward. This indicates that the morphology of the Aβ aggregates is unchanged but their average molecular weight is somewhat larger.

Scattering data, presented as Kratky plots, for solutions of Aβ with hybrid peptides were compared to data for solutions of Aβ with the corresponding recognition peptide (Figure 5). For this comparison, the effect of 15−25-K_6 on Aβ aggregate size and morphology was compared to the effect of 18−25, since 16−25 was insoluble. The effect of hybrid peptides on Aβ aggregates was more variable, and generally more dramatic, than the effect of recognition peptides. A mixture of 20−25-K_6 + Aβ produced a Kratky plot similar in shape and shifted slightly downward from 20−25 + Aβ (Figure 5A). In sharp contrast, inhibitors 15−25-K_6, 16−20-K_6, and 16−20S-K_6 caused drastic changes in the Kratky plots, with the appearance of a distinct peak

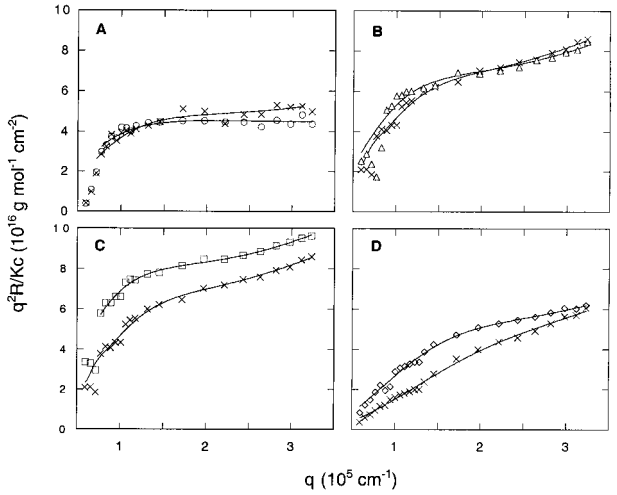

FIGURE 4: Effect of recognition peptides on scattering intensity of Aβ aggregates. Data are presented in the form of Kratky plots (see text). In each case, scattering data were collected 24 h after sample preparation, at 0.5 mg/mL Aβ and 2:1 peptide:Aβ molar ratio. Data for Aβ with recognition peptide is compared to Aβ alone. Aβ curves differ somewhat in each panel, likely due to inaccuracies in concentration determination, which are highly magnified due to the strong concentration dependence of the aggregation. Data are compared for samples prepared at the same or similar times. (A) Aβ (×) or Aβ + 20−25 (○). (B) Aβ (×) or Aβ + 18−25 (Δ). (C) Aβ (×) or Aβ + 16−20 (□). (D) Aβ (×) or Aβ + 16−20S (◇).

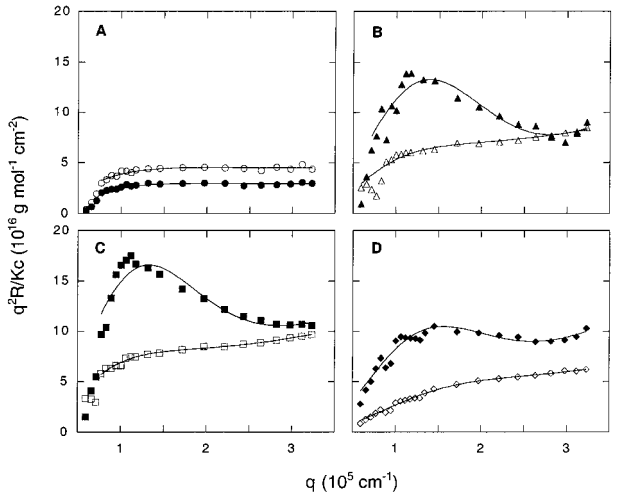

FIGURE 5: Effect of hybrid peptides on scattering intensity of Aβ aggregates. Data are presented in the form of Kratky plots (see text). In each case, the Aβ concentration was 0.5 mg/mL and scattering data were collected 24 h after sample preparation (7 h for Aβ + 16−20-K_6). Peptide:Aβ molar ratio was 2:1 for all samples except Aβ + 16−20-K_6 and Aβ + 16−20S-K_6, where the ratio was 0.5:1. Data for Aβ prepared with recognition peptides is compared to data for Aβ with hybrid peptides. (A) Aβ + 20−25 (○) or Aβ + 20−25-K_6 (●); (B) Aβ + 18−25 (△) or Aβ + 15−25-K_6 (▲); (C) Aβ + 16−20 (□) or Aβ + 16−20-K_6 (■); (D) Aβ + 16−20S (◇) or Aβ + 16−20S-K_6 (◆).

at intermediate values of q (Figure 5B−D). The shape of the curve is consistent with a branched morphology; in particular, the peak can be considered as diagnostic of a loose, branched structure as opposed to a linear fibril or a compact globular structure (*36*). The effect of 16−20-K_6 and 16−20S-K_6 is all the more dramatic, as these data were taken at a 4-fold lower peptide concentration (0.5:1 peptide:Aβ molar ratio) than any of the other data, and the data for 16−20-K_6 + Aβ were collected after only 7 h versus 24 h for

Table 3: Effect of Hybrid Peptides on the Size and Morphology of Aβ Aggregates

added peptide	M_w[a] (× 10^6 Da)	L_c (nm)	l_k (nm)	f
20−25	11 ± 4	2400 ± 700	110 ± 40	NA[b]
20−25-K_6	8 ± 3	2500 ± 600	110 ± 40	NA
18−25	11 ± 1	1100 ± 100	170 ± 30	NA
15−25-K_6	20 ± 3	2000 ± 900	170 ± 70	6 ± 3
16−20	18 ± 1	1500 ± 100	170 ± 20	NA
16−20-K_6	30 ± 5	2500 ± 1300	130 ± 70	6 ± 3
16−20S	3.8 ± 0.3	510 ± 30	190 ± 30	NA
16−20S-K_6	14 ± 2	1300 ± 500	190 ± 30	4 ± 2

[a] M_w, L_c, and l_k, or M_w, L_c, l_k, and f, were determined by fitting eq 2 or 3, respectively, to the data in Figures 4 and 5. For the branching morphology, $L_c = fL_{c,a}$, where $L_{c,a}$ is the length of an individual "arm". [b] NA, not applicable. Data were fit to the linear semiflexible model, eq 2, which does not include a branching variable. Data sets with 16−20-K_6, 15−25-K_6, and 16−20S-K_6 could not be reliably fit to the linear model, justifying the use of the additional model parameter.

all other samples. These results correlate well with observations made by dynamic light scattering (Figure 3): the three hybrid compounds that dramatically changed the fibril shape also caused a sharp increase in apparent growth rate, while those compounds that did not affect aggregation kinetics did not cause a change in aggregate morphology. Thus, in terms of their impact on Aβ aggregate size and morphology, the hybrid peptides are ranked in the order 16−20-K_6 > 16−20S-K_6 > 15−25-K_6 ≫ 20−25-K_6.

To provide additional insight into the changes in size and morphology of the aggregates, we modeled the data using a particle scattering factor of a semiflexible (wormlike) chain or a semiflexible star. Characteristic parameters of the aggregate size and shape, including the contour length L_c, stiffness l_k, molecular weight M_w, and extent of branching f were determined by fitting eqs 2 or 3 to the data. The fitted curves are shown in Figures 4 and 5, and summaries of the fitted parameters are given in Tables 2 and 3.

All of the data for solutions containing a recognition peptide and Aβ could be modeled as linear semiflexible chains. None of the recognition peptides caused a statistically significant change in the stiffness of the fibrils, as quantified by l_k. Recognition peptides 20−25 and 18−25 did not cause a significant change in M_w of Aβ aggregates. The data may suggest an increase in the average fibril length for 20−25 + Aβ mixtures relative to Aβ alone. However, determination of L_c is highly correlated to l_k, and the product $L_c l_k$ for 20−25 + Aβ and Aβ alone are not statistically distinct. Thus, we suspect that this apparent difference in fibril length is not significant and that neither 20−25 nor 18−25 alters the average Aβ fibril length. Both M_w and L_c increased by about a factor of 2 for 16−20 + Aβ and for 16−20S + Aβ relative to Aβ alone. The fact that M_w and L_c increased in parallel indicates that the fibril thickness was not changed.

No statistically significant difference in aggregate molecular weight, aggregate shape, or fibril length was observed for 20−25-K_6 + Aβ compared to 20−25 + Aβ (Table 3). However, dramatic changes in aggregate morphology and increases in average molecular weight were observed with addition of the hybrid peptides 15−25-K_6, 16−20S-K_6, and 16−20-K_6 to Aβ. None of these data sets could be fitted to the semiflexible linear chain model, eq 2. Therefore, the star model, eq 3, which includes a branching parameter, was used to fit the data. M_w increased 2−3-fold for these three hybrid peptides relative to their recognition peptide. The extent of branching f was similar for all three hybrids. The sum of the lengths of the individual "arms" of the branched structure, L_c, generally was greater than for Aβ alone or with recognition peptides.

Results from biophysical and biological assessment of the interaction of recognition and hybrid peptides on Aβ can now be compared. Of the recognition peptides, 16−20 was the only one that provided some protective effect in the MTT toxicity assay and caused a change, albeit modest, in Aβ aggregate size. Peptide 20−25-K_6 was the weakest inhibitor of toxicity of the four hybrid peptides tested and caused little change in Aβ aggregation. Peptide 15−25-K_6 possessed somewhat better protective characteristics and engendered a substantial change in both the rate of aggregation and the aggregate morphology. The two hybrid peptides that provided the strongest protection against Aβ toxicity, 16−20-K_6 and 16−20S-K_6, also elicited the greatest changes in Aβ aggregation.

DISCUSSION

Evidence is mounting that aggregation of Aβ into fibrils, and deposition of fibrils into amyloid plaques, are key steps in the onset and progression of Alzheimer's disease. Details of the pathway by which Aβ monomers are converted to fibrils are still under investigation; available data support a general view that random coil Aβ monomers undergo reversible association into a β-sheet structured oligomer, that fibril growth proceeds via a nucleation and elongation mechanism, and that both electrostatic and hydrophobic interactions play roles in the rate of fibril growth (see refs *41* for review). Compounds that disrupt the amyloid cascade are of interest for two reasons. First, they serve as useful probes of the molecular mechanisms underlying amyloid formation and pathology. Second, they may provide lead compounds for the development of therapeutics. Given these benefits, we set out to develop a strategy that could generate a library of compounds with the desired attributes.

Several groups, including ours, are pursuing the idea that the Aβ sequence itself may provide insight into devising molecules that interrupt Aβ−Aβ self-association. For example, Tjernberg et al. (*27*) explored the possibility of using Aβ fragments to bind to key regions of Aβ and compete with Aβ−Aβ binding. The sequence KLVFF was suggested to bind to Aβ and to inhibit fibril formation. Hughes et al. (*29*) made a conservative Phe → Thr substitution at positions 19 and 20 in designing the peptide QKLVTTAE and observed weak binding and fibril disruption. Soto et al. (*30*) further altered the basic binding domain by substituting prolines at one or more positions and identified several peptides that inhibited fibril formation, as measured by ThT fluorescence. Proline was chosen as a substituent because it is a β-sheet breaker. In all these cases, the functions of binding and of fibril formation disruption are incorporated into the same domain of the compound.

We too realized that fragments of Aβ itself could serve as templates for the design of molecules that recognize Aβ. In contrast to related approaches, however, we pursued a strategy in which the binding and disrupting functions were contained in separate, adjacent regions of the compound. We demonstrated the utility of this strategy for a single com-

pound in previous work (*32*). This modular design format allows optimization of each function of the compound independently, providing a basis for increasing compound activity. Here, we focused our attention on further refinement and optimization of the recognition region of the compounds of interest. The same disrupting domain, hexameric lysine, was used in all cases.

The search for an appropriate recognition element centered on the interior segment of Aβ, as several lines of evidence implicated residues 17−23 of Aβ in fibril formation (*42*−*46*). Our previous studies revealed that a sequence encompassing this region, Aβ(15−25), could serve as an effective recognition element (*32*). We explored the scope of the recognition element with two objectives: (1) to determine whether the recognition element alone could interfere with Aβ aggregation and (2) to ascertain the minimal sequence required for specific recognition. We therefore synthesized a series of 4−8-mer peptides with overlapping sequences, including 16−19, 16−20, 16−25, 17−20, 18−25, 19−25, and 20−25.

Since the mechanism by which Aβ aggregation and Aβ toxicity are linked is not yet established, evaluation of putative Aβ inhibitors preferably includes both biophysical and biological assessment. Biophysical methods used to detect and measure disruption of Aβ aggregation by peptidyl inhibitors include electron microscopy (*27*) and thioflavin T (ThT) fluorescence (*30*). Electron microscopy is useful for visualizing changes in aggregate morphology but provides only limited information about the aggregation event and is difficult to quantify. ThT is a fluorescent marker that recognizes the cross-β structural motif of amyloid fibrils; fluorescence intensity of the dye is reportedly a linear function of the mass of amyloid (*47*). One potential difficulty with the use of ThT fluorescence as an indicator of a compound's inhibitory activity is that a decrease in fluorescence intensity could occur if the test compound blocks ThT binding to amyloid or quenches ThT fluorescence rather than directly blocking amyloid formation. In preliminary studies, we found that ThT was fluorescent in the presence of aggregated Aβ and that our compounds caused little or no reduction in fluorescence intensity. We chose to employ laser light scattering as a means to characterize the interactions of the peptides with Aβ in solution. This technique requires no probe molecules or labels that could potentially interfere with Aβ aggregation. Analysis of scattered light from particles in a solution illuminated by a coherent light source provides a means for monitoring macromolecular association in solution in real time (*48*); the method differs fundamentally from turbidity assays. The data are heavily weighted toward larger particles; thus the method is most sensitive to the species of most interest—aggregated Aβ. Furthermore, quantitative information on changes in the average size and morphology of particles is readily extracted from the data. It should be noted that light scattering does not directly measure the mass of amyloid.

We first tested whether peptides containing only recognition elements alter Aβ aggregation. Peptides 18−25 and 20−25 had no effect on Aβ aggregation kinetics, aggregate size, or aggregate morphology (Figures 3 and 4, Table 2). Peptides 16−20 and 16−20S caused modest changes in aggregate size after 24 h of incubation: the average molecular weight and length of Aβ fibrils roughly doubled in the presence of a 2:1 molar excess of 16−20 or 16−20S, but there was no change in aggregate morphology. The differing effect of 20−25 or 18−25 versus 16−20 or 16−20S suggests that the hydrophobic tripeptide LVF (residues 17−19) constitutes the key recognition feature. The scrambled sequence peptide 16−20S contains the hydrophobic tripeptide VLF at the N-terminus; since both valine and leucine have branched nonpolar side chains and similar hydropathies, the L ↔ V switch is quite conservative. Taken together, these data identify the sequence KLVFF and related sequences as capable of interacting with Aβ, in general agreement with other published results (*27*, *28*), and thus support the choice of these sequences as recognition elements in the design of hybrid compounds.

There are several possible mechanisms by which 16−20 (and 16−20S) could increase the growth rate of fibrils. For example, 16−20 could facilitate the addition of Aβ to a growing fibril, perhaps by stabilizing a transitory conformation required for addition. Alternatively, 16−20 could be incorporated into the elongating fibril, with the increase in weight and length simply a result of an increase in the concentration of material available for addition to the fibril. Or, 16−20 could decrease the rate of fibril initiation, which would result in longer, but fewer, fibrils. The data are insufficient to discriminate between these and other hypotheses; the mechanism of interaction of 16−20 with full-length Aβ is under further investigation.

Next, we set out to evaluate the effect, if any, of the disrupting element on Aβ aggregation. To test this we synthesized a panel of hybrid peptides, utilizing three overlapping Aβ fragments (15−25, 16−20, or 20−25) or a scrambled fragment (16−20S) as recognition elements, and a polar hydrophilic lysine hexamer string as a putative disrupting element. Three of the four hybrid peptides, those that contained LVF or a related sequence (15−25-K_6, 16−20-K_6, and 16−20S-K_6), caused a dramatic increase in the aggregation kinetics of Aβ, as assessed by dynamic light scattering (Figure 3), and a definite change in aggregate size and morphology, as determined by static light scattering (Table 3, Figure 5). These results stand in sharp contrast to the small changes elicited with the recognition peptides alone. Peptides 16−20-K_6 and 16−20S-K_6 were active at lower molar ratios than 15−25-K_6. The fourth hybrid peptide, 20−25-K_6, did not cause a measurable change in Aβ aggregation compared to the recognition peptide 20−25 (Figure 5). Thus, the biophysical changes occurring upon addition of the hybrid peptide cannot be attributed simply to a nonspecific effect of the lysine hexamer. These results identify 16−20-K_6 as the most potent modulator of Aβ aggregation.

These studies indicate distinct and significant roles for both the recognition and disrupting elements. Recognition peptides such as KLVFF, which lack a disrupting domain, cause at most subtle changes in Aβ aggregation. On the other hand, molecules with a disrupting domain but no competent recognition element are unable to alter the kinetics of Aβ aggregation or the morphology of the resulting aggregates. For example, 20−25 was unable to serve as an effective recognition element alone (Table 2, Figure 4A), and the hybrid peptide possessing this recognition element, 20−25-K_6, was similarly ineffective (Figure 5A). Moreover, the addition of this polar sequence to 16−20 leads to a molecule of diminished activity, as seen by the reduced potency of

15−25-K_6 relative to 16−20-K_6. The hybrid peptide 16−20S-K_6, in which the scrambled recognition element VLFKF is employed, also displayed significant activity. Taken together, these data identify the hydrophobic tripeptide LVF (VLF) as a potent recognition element and highlight a crucial role for the disrupting domain.

The pronounced changes elicited by the active hybrid peptides include increases in the kinetics of aggregation (Figure 3), increases in the average molecular weights of the aggregates (Table 3), and alterations in the morphology of the resulting aggregates from linear to branched (Figure 5). It is important to note here that the wormlike star model is useful for comparative analysis of the data but is not likely to provide a completely accurate physical picture of the Aβ aggregates. "Branching" in this case could indicate that the compounds disrupt the normal linear elongation of the fibrils and provide a locus for continued growth in more than one dimension. Alternatively, it could be a sign of increased fibril−fibril association, leading to an entangled web of fibrils. It is unlikely that the basic fibrillar structure is perturbed, since the persistence length (a measure of fibril flexibility) and the ratio M_w/L_c (related to the fibril cross-sectional area) are not dramatically altered. The molecular basis for these changes is currently unknown, but studies aimed at addressing this issue may provide insight into the design of improved inhibitors.

The observed changes in fibril formation in the presence of the various peptides prompted us to examine their effects on the cellular toxicity of Aβ. For this purpose, the MTT reduction assay using the neuronal cell line, PC-12, was employed. This assay has been used by a number of groups as a measure of Aβ toxicity (*10*, *40*, *49*). The toxicity of Aβ as measured by MTT reduction depends on aggregation of Aβ into fibrils (*40*), indicating that this assay reports on features that may be relevant to the physiological action of Aβ. Of the recognition peptides tested, only 16−20 and 16−19, both of which contain the LVF motif, inhibited Aβ toxicity at a 2:1 peptide:Aβ molar ratio. Addition of the disrupting element enhanced the potency of 16−20; 16−20-K_6 was significantly more effective at ameliorating Aβ toxicity than was the recognition peptide alone. Results from the cellular toxicity assays strongly correlated with observations from the biophysical investigations: those compounds that were most protective in the cellular assay also elicited the largest changes in Aβ aggregation. These data further demonstrate that the best inhibitory activity is achieved with compounds containing both the LVF recognition element and an active disrupting element.

An intriguing result of this investigation is that the best inhibitors, as measured by protection from toxicity, appear to alter Aβ aggregation by increasing the rate of aggregation and altering aggregate morphology. This mechanism differs from those reported by other groups, in which investigations focused on discovering molecules that block aggregation. Agents that alter rather than block aggregation, such as those reported here, may have therapeutic advantages. For example, such agents may be preventative at lower molar ratios, as their model of function does not require that they sequester all or the majority of Aβ monomer present. Indeed, preliminary experiments in our laboratory indicate that 16−20-K_6 inhibits Aβ(1−39) toxicity down to a 1:4 peptide:Aβ molar ratio or perhaps lower. In addition, the mode of action of these compounds provides the basis for new insights into the mechanisms of Aβ toxicity. Our data provide indirect support for the hypothesis that small soluble oligomers, rather than large fibrillar deposits, are the toxic Aβ species (*50*, *51*).

ACKNOWLEDGMENT

Kari Kaiser assisted with analytical ultracentrifugation experiments.

REFERENCES

1. Kang, J., Lemaire, H. G., Unterbeck, A., Salbaum, J. M., Masters, C. L., Grzeschik, K. H., Multhaup, G., Beyreuther, K., and Muller-Hill, B. (1987) *Nature 325*, 733−736.
2. Joachim, C. L., and Selkoe, D. J. (1992) *Alzheimer Dis. Assoc. Disord. 6*, 7−34.
3. John, V., Latimer, L. H., Tung, J. S., and Dappen, M. S. (1997) *Annu. Rep. Med. Chem. 32*, 11−20.
4. Games, D., Adams, D., Alessandrini, R., Barbour, R., Berthelette, P., Blackwell, C., Carr, T., Clemens, J., Donaldson, T., Gillespie, F., Guido, T., Hagopian, S., Johnson-Wood, K., Khan, K., Lee, M., Leibowitz, P., Lieberburg, I., Little, S., Masliah, E., McConlogue, L., Montoya-Zavala, M., Mucke, L., Paganini, L., Penniman, E., Power, M., Schenk, D., Seubert, P., Snyder, B., Soriano, F., Tan, H., Vitale, J., Wadsworth, S., Wolozin, B., and Zhao, J. (1995) *Nature 373*, 523−527.
5. Moran, P. M., Higgins, L. S., Cordell, B., and Moser, P. C. (1995) *Proc. Natl. Acad. Sci. U.S.A. 92*, 5341−5345.
6. Hsiao, K., Chapman, P., Nilsen, S., Eckman, C., Harigaya, Y., Younkin, S., Yang, F., and Cole, G. (1996) *Science 274*, 99−102.
7. Johnson-Wood, K., Lee, M., Motter, R., Hu, K., Gordon, G., Barbour, R., Khan, K., Gordon, M., Tan, H., Games, D., Lieberburg, I., Schenk, D., Seubert, P., and McConlogue, L. (1997) *Proc. Natl. Acad. Sci. U.S.A. 94*, 1550−1555.
8. Pike, C. J., Walencewicz, A. J., Glabe, C. G., and Cotman, C. W. (1991) *Eur. J. Pharmacol. 207*, 367−368.
9. Busciglio, J., Lorenzo, A., and Yankner, B. A. (1992) *Neurobiol. Aging 13*, 609−612.
10. Iversen, L. L., Mortishire-Smith, R. J., Pollack, S. J., and Shearman, M. S. (1995) *Biochem. J. 311*, 1−16.
11. Polvikoski, T., Sulkava, R., Haltia, M., Kainulained, K., Vuorio, A., Verkkoniemi, A., Niinisto, L., Halonenm, P., and Kontula, K. (1995*) N. Engl. J. Med. 333*, 1242−1247.
12. Selkoe, D. J. (1997) *Science 275*, 630−631.
13. Simmons, L. K., May, P. C., Tomaselli, K. J., Rydel, R. E., Fuson, K. S., Brigham, E. F., Wright, S., Lieberburg, I., Becker, G. W., Brems, D. N., and Li, W. (1994) *Mol. Pharmacol. 45*, 373−379.
14. Pike, C. J., Walencewicz, A. J., Glabe, C. G., and Cotman, C. W. (1991) *Brain Res. 563*, 311−314.
15. Pike, C. J., Burdick, D., Walencewicz, A. J., Glabe, C. G., and Cotman, C. W. (1993*) J. Neurosci. 13*, 1676−1687.
16. Schenk, D. B., Rydel, R. E., May, P., Little, S., Panetta, J., Lieberburg, I., and Sinha, S. (1995) *Med. Chem. 38*, 4141−4154.
17. Lansbury, P. T. (1997) *Curr. Opin. Chem. Biol. 1*, 260−267.
18. Pollack, S. J., Sadler, I. I. J., Hawtin, S. R., Tailor, V. J., and Shearman, M. S. (1995) *Neurosci. Lett. 197*, 211−214.
19. Sadler, I. J., Smith, D. W., Shearman, M. S., Ragan, C. I., Tailor, V. J., and Pollack, S. J. (1995) *Neuroreport 7*, 49−53.
20. Kisilevsky, R., Lemieux, L. J., Fraser, P. E., Kong, X., Hultin, P. G., and Szarek, W. A. (1995) *Nat. Med. 1*, 143−148.
21. Lomakin, A., Chung, D. S., Benedek, G. B., Kirschner, D. A., and Teplow, D. B. (1996) *Proc. Natl. Acad. Sci. U.S.A. 93*, 1125−1129.
22. Wood, S. J., MacKenzie, L., Maleeff, B., Hurle, M. R., and Wetzel, R. (1996) *J. Biol. Chem. 271*, 4086−4092.
23. Tomiyama, T., Shoji, A., Kataoka, K.-I., Suwa, Y., Asano, S., Kanetko, H., and Endo, N. (1996) *J. Biol. Chem. 271*, 10205−10208.

24. Esler, W. P., Stimson, E. R., Ghilardi, J. R., Felix, A. M., Lu, Y.-A., Vinters, H. V., Mantyh, P. W., and Maggio, J. E. (1997). *Nat. Biotechnol. 15*, 258−263.
25. Waite, J., Cole, G. M., Frautschy, S. A., Connor, D. J., and Thal, L. J. (1992) *Neurobiol. Aging 13*, 595−599.
26. Camilleri, P., Haskins, N. J., and Howlett, D. R. (1994) *FEBS Lett. 341*, 256−258.
27. Tjernberg, L. O., Naslund, J., Lindqvist, F., Johansson, J., Karlstrom, A. R., Thyberg, J., Terenius, L., and Nordstedt, C. (1996) *J. Biol. Chem. 271* (*15*), 8545−8548.
28. Tjernberg, L. O., Lilliehöök, C., Callaway, D. J. E., Näslund, J., Hahne, S., Thyberg, J., Terenius, L., and Nordstedt, C. (1997) *J. Biol. Chem. 272*, 12601−12605.
29. Hughes, S. R., Goyal, S., Sun, J. E., Gonzalez-DeWhitt, P., Fortes, M., Riedel, N. G., and Sahasrabudhe, S. R. (1996) *Proc. Natl. Acad. Sci. U.S.A. 93*, 2065−2070.
30. Soto, C., Kindy, M. S., Baumann, M., and Frangione, B. (1996) *Biochem. Biophys. Res. Commun. 226*, 672−680.
31. Soto, C., Sigurdsson, E. M., Morelli, L., Kumar, R. A., Castano, E. M., and Frangione, B. (1998) *Nat. Med. 4*, 822−826.
32. Ghanta, J., Chen, C.-L., Kiessling, L. L., and Murphy, R. M. (1996) *J. Biol. Chem. 271*, 29525−29528.
33. Shen, C.-L., Fitzgerald, M. C., and Murphy, R. M. (1994) *Biophys. J. 65*, 2383−2395.
34. K.oppel, D. E. (1972) *J. Chem. Phys. 57*, 4814−4820.
35. Shen, C.-L., and Murphy, R. M. (1995) *Biophys. J. 69*, 640−651.
36. Burchard, W. (1983) *Adv. Polym. Sci. 48*, 1−124.
37. Koyama, R. (1973) *J. Phys. Soc. Jpn. 34*, 1029−1038.
38. Huber, K., and Burchard, W. (1989) *Macromolecules 22*, 3332−3336.
39. Stewart, W. E., and Sorensen, J. P. (1981) *Technometrics 23*, 131−141.
40. Shearman, M. S., Ragan, C. I., and Iverson, L. L. (1994) *Proc. Natl. Acad. Sci. U.S.A. 91*, 1470−1474.
41. Harper, J. D., and Lansbury, P. T., Jr. (1997) *Annu. Rev. Biochem. 66*, 385−407.
42. Fraser, P. E., Nguyen, J. T., Surewicz, W. K., and Kirschner, D. A. (1991) *Biophys. J. 60*, 1190−1201.
43. Hilbich, C., Kisters-Woike, B., Reed, J., Masters, C. L., and Beyreuther, K. (1992) *J. Mol. Biol. 228*, 460−473.
44. Terzi, E., Hölzemann, G., and Seelig, J. (1995) *J. Mol. Biol. 252*, 633−642.
45. Lee, J. P., Stimson, E. R., Ghilardi, J. R., Mantyh, P. W., Lu, Y.-A., Felix, A. M., Llanos, W., Behbin, A., Cummings, M., Van Criekinge, M., Timms, W., and Maggio, J. E. (1995) *Biochemistry 34*, 5191−5200.
46. Wood, S. J., Wetzel, R., Martin, J. D., and Hurle, M. R. (1995) *Biochemistry 34*, 724−730.
47. Naiki, H., and Nakakuki, K. (1996) *Lab. Invest. 74*, 374−382.
48. Murphy, R. M. (1997) *Curr. Opin. Biotechnol. 8*, 25−30.
49. Hertel, C., Hauser, R., Schubenel, R., Seilheimer, B., and Kemp, J. A. (1996) *J. Neurochem. 67*, 272−6.
50. Lambert, M. P., Barlow, A. K., Chromy, B. A., Edwards, C., Freed, R., Liosatos, M., Morgan T. E., Rozovky, I., Trommer, B., Viola, K. L., Wals, P., Zhang, C., Finch, C. E., Krafft, G. A., and Klein, W. L. (1998) *Proc. Natl. Acad. Sci. U.S.A. 95*, 6448−6453.
51. Wujek, J. R., Dority, M. D., Frederickson, R. C. A., and Brunden, K. R. (1996) *Neurobiol. Aging 17*, 107−113.

BI982119E